

## Seismic anisotropy in the south western Pacific region from shear wave splitting

Eszter Király,<sup>1,2</sup> Irene Bianchi,<sup>1</sup> and Götz Bokelmann<sup>1</sup>

Received 1 December 2011; revised 28 January 2012; accepted 1 February 2012; published 2 March 2012.

[1] We perform shear-wave splitting measurements to determine seismic anisotropy in the upper mantle under the remote and still not well-understood South Western Pacific Region, more precisely the New Hebrides subduction zone. We obtained 29 good and 35 fair splitting measurements at 8 stations and 93 good and fair Null measurements from the data provided by various networks. According to the splitting parameters, the seismic stations are grouped into “eastern” and “western” stations. Anisotropy of the subducting plate (“western” stations) appears to be the result of absolute plate motion (APM) of the Australian plate. From fast orientations alone, it would be difficult to judge which process is responsible for the anisotropic structure: either the absolute plate motion or trench-parallel “toroidal” flow. Their delay times reveal that these anisotropic parameters can be explained without the presence of the subduction zone, and the APM provides a simple explanation for the observed anisotropy. On the other hand, delay times at “eastern” stations are higher than that of “western” stations. These stations are located close to the subduction zone, and the nearly trench-parallel orientation of fast polarization axes and their higher splitting delay times indicate the presence of subduction zone. Anisotropy at “eastern” stations is apparently due to the additional effect from “toroidal” flow near the subduction zone, which increases the total anisotropy.

**Citation:** Király, E., I. Bianchi, and G. Bokelmann (2012), Seismic anisotropy in the south western Pacific region from shear wave splitting, *Geophys. Res. Lett.*, 39, L05302, doi:10.1029/2011GL050407.

### 1. Introduction

[2] Seismic anisotropy can provide information about past and current deformation in the Earth’s interior remotely from the surface. One of the most popular techniques to reveal the presence of seismic anisotropy is the analysis of shear-wave splitting. A seismic shear wave that propagates through an anisotropic region of the Earth splits into two waves with different velocities and polarization. Local S-waves as well as teleseismic SKS, SKKS and core-reflected ScS phases may be used for investigations. We used SKS and SKKS waves since they give strong constraints; the measured splitting is interpreted in terms of two parameters, fast polarization direction and delay between the two shear waves [e.g., *Silver and Chan*, 1988], which constrain the

spatial orientation of the anisotropic structure at depth, and its thickness [*Babuska and Cara*, 1991].

[3] Mantle seismic anisotropy observed in seismic recordings indicates anisotropy in the subsurface at spatial scales of tens to hundreds of kilometers. That macroscopic anisotropy generally results from mineral properties at microscopic scales, through lattice-preferred alignment of minerals during deformation, especially of olivine. At upper mantle conditions (relatively low pressure and water-poor), the A-type olivine fabric is generally considered, for which seismic fast polarization axes are oriented parallel to the shear plane of mantle flow. However, experiments in laboratory reveal that under high stress and high water content conditions the orientation of olivine may change. *Jung and Karato* [2001] have introduced the A-, B- and C-type olivine highlighting that at high stress and at high water content olivine [001] (c)-axis can be sub-parallel to the shear direction, rather than the a-axis.

[4] Shear-wave splitting observations generally present particular orientations in (oceanic) subduction zones, namely trench-parallel or trench-perpendicular: for instance, trench-normal splitting orientations were found at Izu-Bonin [*Fouch and Fischer*, 1998] and in Japan [*Nakajima and Hasegawa*, 2004], trench-parallel orientation behind the slab in the Tonga Subduction Zone [*Foley and Long*, 2011], trench-parallel orientation in the mantle wedge in Lau Basin [*Smith et al.*, 2001]. Which processes generate these patterns of anisotropy are still under debate, because of the contribution of several factors, such as the different morphology of the subducting lithosphere, the particular PT conditions, or the geodynamic history [e.g., *Long and van der Hilst*, 2005]. *Long and Silver* [2008] give an overview of shear-wave splitting measurements of 13 subduction zones from all over the world and discuss global trends of splitting behavior in order to determine dominant properties of the subduction zone flow field. They characterized the wedge and sub-wedge region separately comparing local and teleseismic S-wave measurements. In most cases the sub-wedge anisotropic signal is simple: anisotropy orientation is trench-parallel (except Cascadia), delay times ( $\delta t$ ) appear to increase with trench migration velocity. Mantle wedge flow is more complicated since flow is the resultant of competing trench-perpendicular 2D corner flow and trench-parallel 3D flow induced by trench migration. Fast orientations and values of  $\delta t$  are more variable and conditions of the wedge increase the probability of the presence of B-type fabric. SKS shear-wave splitting constrains well the strength of anisotropy, however it does not give information about its depth location. Since the lower mantle appears to be isotropic and anisotropy of D" layer and that of transition zone might be patchy [*Savage*, 1999] we consider that anisotropic signal reflects deformation in the upper mantle.

<sup>1</sup>Institute of Meteorology and Geophysics, Universität Wien, Vienna, Austria.

<sup>2</sup>Laboratoire de Géologie, École Normale Supérieure, Paris, France.

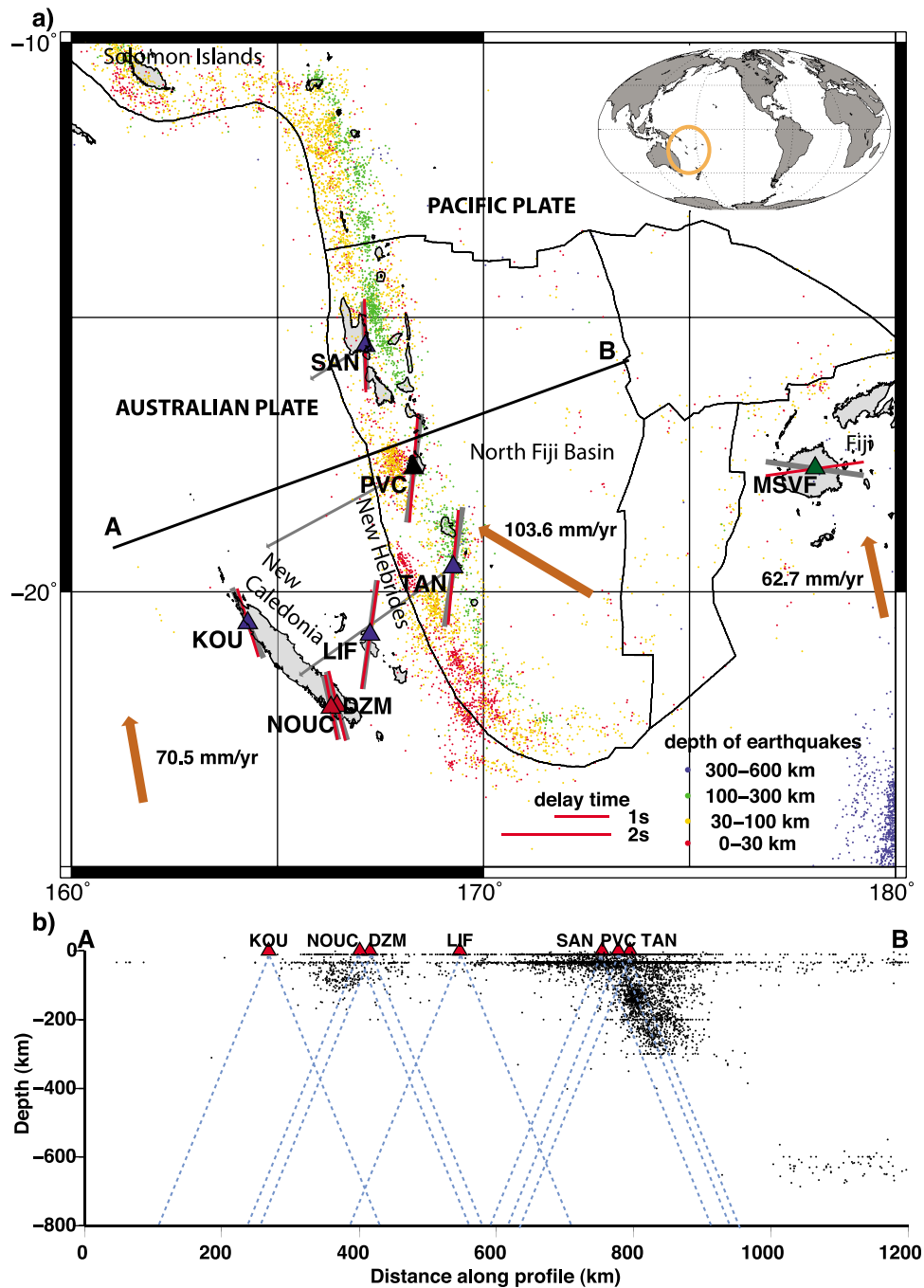


**Figure 1.** (a) Map of the study area, with location of seismic stations. Results of shear-wave splitting are represented for each station, with mean (red) and median (grey) values of individual measurements. Brown arrows indicate plate motion. Subducting slab is defined by seismicity, colors correspond to depth. Stations and networks are described in Table S1. Grey arrows are the GPS measurements (see Table S4 for azimuth direction and velocity) from *Taylor et al.* [1995] of the new Hebrides plate vs Australian Plate. (b) Vertical cross section along the line AB (azimuth = 70°). Grey dots represent seismicity from 2000 until 2011. Red triangles indicate stations at the surface. Blue lines give ray paths shown with maximum incidence angles at each station (horizontal exaggeration).

[5] This work focuses on seismic anisotropy around the New Hebrides subduction zone situated to the east of Australia (Figure 1). The subduction is located between New Caledonia and the islands of the New Hebrides where the Australian plate is subducting eastward under the Pacific plate. This region exhibits complicated geodynamical features, resulting from its evolution during the past 100 My.

The boundary of the Australian and Pacific plates migrated outwards through the development of a succession of dilatational basins and island arcs, as arcuate submarine ridges and basins concentric to the eastern coast of Australia witness [*Yan and Kroenke*, 1993]. During the Late Miocene (about 10 My), the arrival of an abnormally thick oceanic plateau, (the Ontong Java plateau) caused a drastic change

along the northern part of the boundary: stopping the subduction process near the Solomon islands and forcing part of the Australian plate to subduct in the reverse direction, along the New Hebrides trench.

[6] *Schellart et al.* [2006] give a comprehensive evolution model of the area from the Cretaceous to present days based on geological and geophysical data, but the dynamic processes which shaped this area are not yet well-understood. According to their model, the New Hebrides subduction zone initiated in the last 10 Ma, rolling back to the west with clockwise rotation and opening the wedge-shaped North Fiji Basin. The complex pattern of spreading in the North Fiji Basin might be a result of asymmetric opening. The subduction may have been accompanied by lateral flow of mantle material around the lateral slab edge towards the mantle wedge side. On the mantle wedge side, geochemical studies based on lead isotopes [e.g., *Heyworth et al.*, 2011] suggest a significant trench-parallel flow. The young, fast and deep subduction zone with the unusual asymmetric rotation may create unique structures in the upper mantle.

[7] Few studies were published in that area: *Pillet et al.* [1999] used the surface waves to constrain the 3D structure of the area. According to them this region is characterized by important variations of the phase velocity anomalies, indicating the diverse tectonic regions, which have been strongly deformed. *Barruol and Hoffmann* [1999] and *Fischer and Wiens* [1996] examined the anisotropy under Nouméa and Fiji, respectively. In this study we used 8 stations located close to the New Hebrides Trench. Thus, this is the first comprehensive SKS shear-wave splitting investigation around the New Hebrides Trench.

## 2. Data, Method and Results

[8] A comprehensive data-set from global and local networks has been constructed for this study. Data from the (global) Geoscope and Global Seismograph Network stations (NOUC, DZM, PVC, MSVF) were taken from the database of IRIS (Incorporated Research Institutions for Seismology), while data of the local Cavascope network [*Pillet et al.*, 2008] (KOU, LIF, PVC, SAN, TAN) were provided directly by the Laboratoire de Sismologie - Centre IRD de Nouméa.

[9] Altogether 174 events were used at 8 broadband stations. Geoscope stations provide data from 1988 (NOUC) or from 2003 (DZM) till 2011, data of the GSN station (MSVF) are available from 1994 till 2011, whereas time interval of data from Cavascope network is 1993–1998.

[10] Teleseismic events located at distances in the range of 85° to 140° and of magnitude greater than 6.0 during the whole recording time of the station have been selected, in order to get the largest and best possible quality data. The origin and location of the events are taken from the Harvard CMT catalog (<http://www.globalcmt.org/CMTsearch.html>), and phase arrivals are calculated using the IASP91 model [*Kennett and Engdahl*, 1991].

[11] We measured shear wave splitting using the SKS phase, and for some events, we used the whole SKS+SKKS wave train. These waves enter the outer core, losing information about the previous path, thus every splitting observed at the station is due to the “receiver-side” path in the mantle. Moreover, the initial polarization direction of the SKS phase is known (radial) where it leaves the core. To avoid

complications from converted phases, free-surface effects and phase changes at crustal discontinuities, incidence angles should be steep (critical angle is 35° from the vertical). Otherwise the surface distorts amplitude and phase and generates non-linear particle motion even without the presence of anisotropy [*Savage*, 1999].

[12] The shear-wave splitting parameters (i.e., fast axis polarization azimuth  $\phi$  and delay time  $\delta t$ ) were obtained using the SplitLab software [*Wüstefeld et al.*, 2008]. Synthetic tests showed that the minimum energy method is the most reliable technique for determining the splitting parameters and to distinguish real splitting from Null measurements [*Wüstefeld and Bokelmann*, 2007]. Beside that technique, the rotation-correlation method was always applied to check the quality of the measurements. The individual  $\phi$  and  $\delta t$  results are listed in Table S2 in the auxiliary material and plotted in Figure 2, while mean and median values for each station are summarized in Table 1 and plotted in Figure 1.<sup>1</sup>

[13] We obtained 29 good and 35 fair splitting measurements, as well as 93 good and fair Null measurements at 8 stations. On the western side of the trench, the majority of the data are given by earthquakes from the east and the southeast, which originate from the Chile subduction zone. Beside a large number of Null measurements (93), the events also yield many non-Null splitting measurements. To the east of the trench, the region is characterized by a smaller amount of Nulls, out of 93 Null measurements counted at the 8 stations, SAN, PVC and TAN count 19 Null measurements, while LIF, KOU, DZM and NOUC count 68 Null measurements. The bulk is due to NOUC and DZM, due to their longer recording time. The average ratio of Non-Null vs Null measurements is for the “eastern” stations more than twice larger than for the “western” stations. This difference can be related to a weaker anisotropic signal under the “western” stations (see Table S3). Since on islands and in coastal environments ocean wave activity generates microseismic noise (as given by *Fontaine et al.* [2007]), which can be more energetic than the signal itself, we had sometimes to use strong frequency filters such as a 0.01–0.2 Hz band-pass Butterworth filter.

[14] The results of New Hebrides subduction zone are divided into two groups. The first group is the “western” stations KOU, NOUC and DZM, located to the west of (and behind) the slab. These show  $\phi$  values around  $-20^\circ$  and splitting  $\delta t$  are around 1.3 s. The second group is the “eastern” stations LIF, SAN, PVC, and TAN, located to the east (of and in front of the slab), which show approximately N-S fast orientation and higher delay times ( $\sim 2$  s). The station MSVF instead is considered as belonging to the Tonga subduction zone, it displays an almost E-W polarization of the fast axis with a  $\sim 1.8$  s delay time. That orientation is to be explained in the context of the Tonga subduction zone [*Fischer and Wiens*, 1996], rather than the New Hebrides Trench. We thus treat these data separately.

## 3. Discussion

[15] The strike of the New Hebrides Trench is roughly 160°, so the clearest vertical view of the subduction system

<sup>1</sup>Auxiliary materials are available in the HTML. doi:10.1029/2011GL050407.

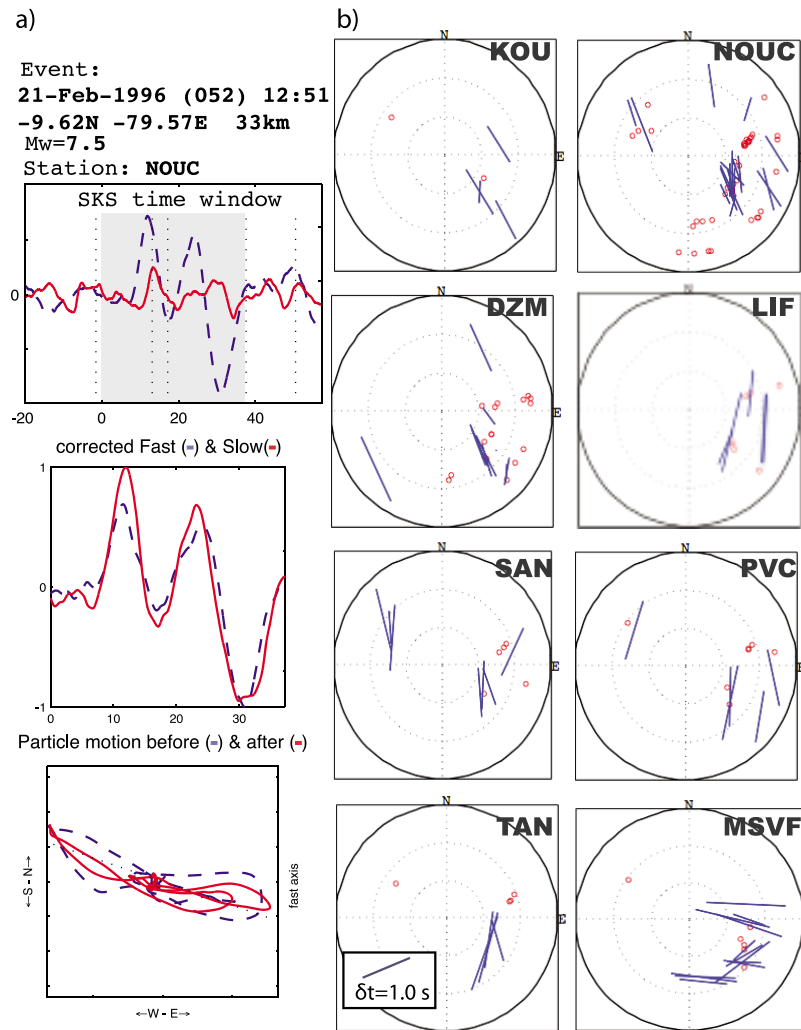


**Figure 2.** (a) Waveform example showing shear-wave splitting for the event on 21st February 1996, recorded at station NUOC (see Table S1), on top North-South and East-West components of the seismogram, in the middle the corrected fast (dashed blue line) and slow (solid red line) components, on bottom the initial (dashed blue line) and corrected (solid red line) particle motions; (b) lower hemispheres under the stations showing individual splitting measurements indicating backazimuthal direction (position of the bar), splitting orientation (orientation of the bar) and delay time (length of the bar).

is given by a cross section with an azimuth of  $70^\circ$ . The vertical cross section (Figure 1b) shows a projection of all earthquakes given by NEIC (National Earthquake Information Center) from 1990 until 2011, and stations onto a line passing through the New Hebrides Trench and the surrounding area (Figure 1a, line AB). Slab geometry is defined by earthquake hypocenters. Seismic activity disappears

around the depth of 350 km till about 500 km. Between 500–700 km depth the earthquake distribution may suggest a flat horizontal piece of slab.

[16] As stated by *Montagner et al.* [2000], anisotropic signal comes from the upper mantle primarily, and in the case of the “western” stations, as shown in Figure 1b the path of the incoming rays does not pass through the

**Table 1.** Splitting Parameters for Each Station

Station Name	Mean of $\Phi$ ( $^\circ$ )	Median of $\Phi$ ( $^\circ$ )	Standard Deviation of $\Phi$ ( $^\circ$ )	Mean of $\delta t$ (s)	Median of $\delta t$ (s)	Standard Deviation $\delta t$ (s)
DZM	-17.6	-22.0	15.0	1.3	1.3	0.6
KOU	-22.5	-31.0	18.4	1.3	1.4	0.4
LIF	11.5	10.0	9.2	2.0	2.0	0.7
NOUC	-14.2	-17.0	17.2	1.2	1.2	0.4
PVC	5.8	10.0	11.8	2.0	2.0	0.3
SAN	-1.1	-3.0	14.8	1.7	1.6	0.4
TAN	6.7	11.5	15.1	2.1	2.2	0.5
MSVF	-96.3	-84	27.5	1.8	1.8	0.6

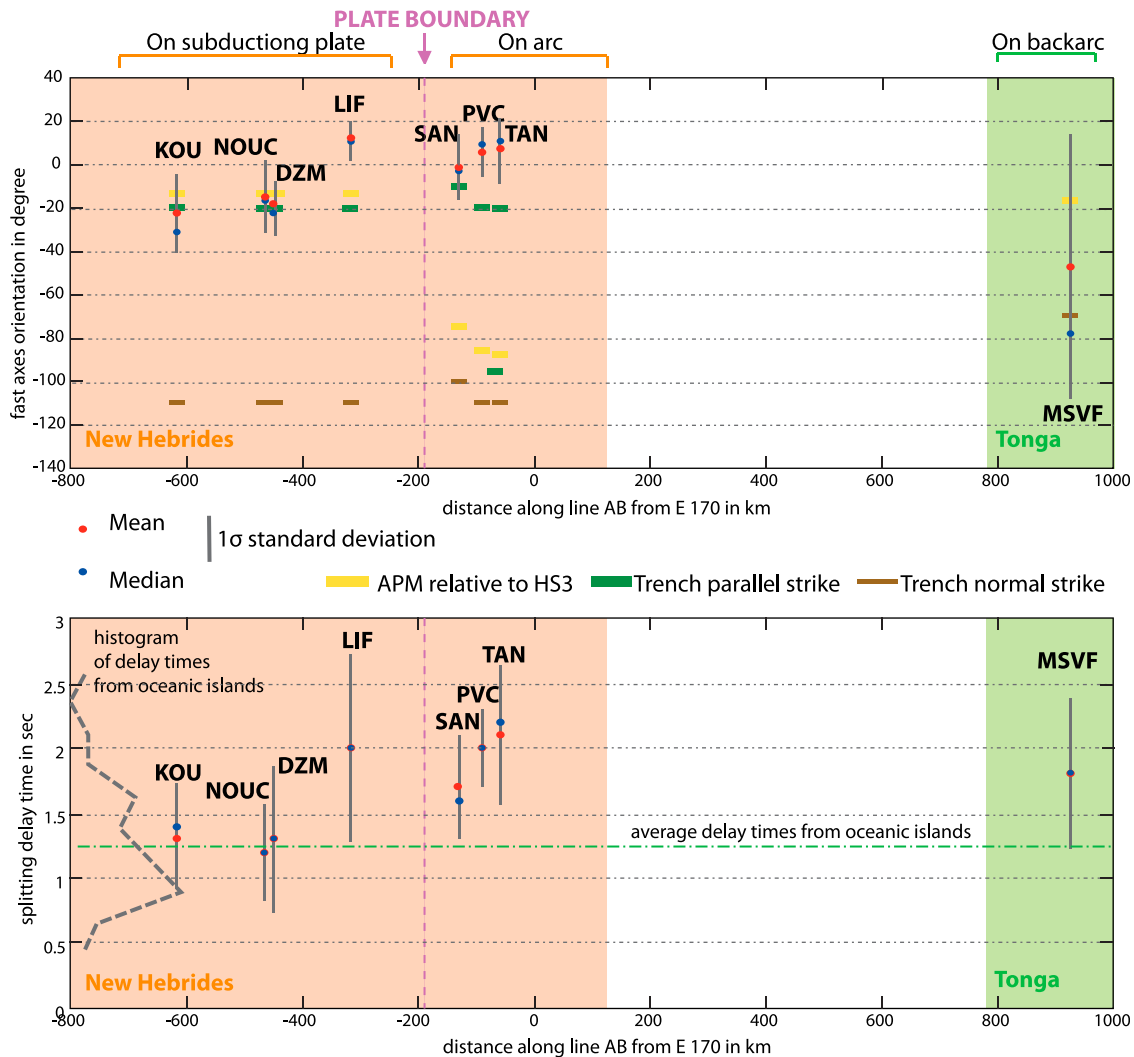


**Figure 3.** (top) Fast orientations and (bottom) splitting delay times, as a function of distance along the cross section AB in Figure 1a. Red and blue dots represent mean and median values, respectively, black bars define the  $1\sigma$  standard deviation. APM, trench-parallel and trench-normal strikes are shown by orange, green and brown bars, respectively. Histogram and average value of delay times from oceanic islands are calculated from the Global Splitting Database (<http://www.gm.univ-montp2.fr/splitting/>) [Wüstefeld *et al.*, 2008].

subduction zone, allowing a simple interpretation of the splitting results as related only to the “undeformed” structures. To the East, the presence of the subduction zone and its influence on the anisotropy symmetry directions becomes more important. Figure 3 summarizes splitting results at all stations and possible interpretations. The first diagram represents fast orientation; the second one represents delay times as a function of distance along the cross section AB (Figure 1b). Red and blue dots represent mean and median values, respectively; black bars define  $1\sigma$  standard deviation. Absolute plate motion (APM) relative to hotspot reference frame (NUVEL-1A HS3 [Gripp and Gordon, 2002]) is determined by the UNAVCO Plate Motion Calculator at each station (<http://www.unavco.org>). APM at KOU, NOUC and DZM located on the Australian plate are calculated directly with Australian plate motion at the appropriate location. GPS measurements of Taylor *et al.* [1995] revealed that Fiji and Loyalty Islands do not move significantly with respect to the Australian plate, thus plate motion at LIF and MSVF stations were determined also by the motion of

Australian plate. SAN, PVC and TAN stations are situated on the New Hebrides micro-plate which is not incorporated in the NUVEL-1A HS3 model. Taylor *et al.* [1995] presented the motion of New Hebrides plate relative to the Australian plate, in this study they used some GPS stations which are not co-located with the seismic stations, but they are close enough that their distance can be neglected at the scale of this study. The combination of motion of New Hebrides plate relative to Australia and of Australia relative to the HS3 hotspot reference model gives the absolute motion of New Hebrides plate relative to HS3 at SAN, PVC and TAN; the vectorial combination of the HS3 Australia motion plus the motion of each station relative to Australia from Taylor *et al.* [1995] were combined to give the motion of the stations relative to HS3 (details for each station in Table S4). Subduction zones often represent trench-parallel or trench-perpendicular orientations, only sometimes oblique orientation [Long and Silver, 2008]. Thus, trench-parallel (green) and trench-normal (brown) orientations are indicated on the diagram.

[17] Since anisotropic signal at all stations comes primary from the sub-slab region (see Figure 1b), where the effect of water is not significant, we consider A-type olivine fabrics. Trench-normal orientations fall far from our results at all stations; our data cannot be explained by a process that creates trench-normal orientation of anisotropy.

[18] In the case of “western” stations, green and orange bars of the top panel of Figure 3 clearly show that both models put forward by *Barruol and Hoffmann* [1999] can explain the fast directions, since APM and trench-parallel orientations are within the  $1\sigma$  standard deviation interval and close to mean values. From fast orientations at these stations it is difficult to distinguish between simple shear induced by absolute plate motion and trench-parallel “toroidal” flow. Inspecting splitting delay times for these stations we find though that they are close to the average delay time value of splitting measurements from oceanic islands. For that comparison, we have taken all stations on oceanic islands from the SplitLab database of *Wüstefeld et al.* [2008], and have calculated the histogram and the average value. The good agreement between splitting delay at “western” stations with typical ocean station values suggests that the anisotropy at these stations can be explained without the presence of the subduction zone. Thus, APM appears to explain the anisotropy observed at the “western” stations.

[19] The delay times of “eastern” stations, are higher than most of the “western” stations. “Eastern” stations are located close to the subduction zone. An obvious candidate for explaining the additional  $\delta t$  is the presence of the subduction zone, in the form of slab-parallel flow, as expected from the return flow around the slab (“toroidal” flow), while the slab is rolling back. APM of the Australian plate and the strike of the subduction are nearly parallel, thus superposition of their effects may create stronger anisotropy. As a consequence, delay times can be expected to be larger at the “eastern” stations. The fast orientations also confirm the notion, since they are nearly trench-parallel. Therefore, anisotropic signal beneath the “eastern” stations might be due to the APM of Australian plate together with the “toroidal” mantle flow behind the subducting slab.

[20] To summarize, anisotropy of “western” stations appears to be produced by the absolute plate motion of the Australian plate while anisotropy beneath the “eastern” stations may show anisotropy associated with the subduction zone. The anisotropy might be due to the combination of APM of Australian plate and the “toroidal” flow behind the slab. The magnitude of the APM calculated is about 70 mm/yr at “western” stations (Table S5) and the northernmost of the “eastern” stations, SAN (Table S4). The delay time is considerably faster for the two southeastern stations PVC and TAN, due to the plate motion. At these two stations, the splitting is particularly strong.

[21] Beside this simple interpretation of the most striking features in the results, there is a secondary feature which is yet unexplained, namely the slight deviation from trench-parallel orientation at the “eastern” stations. Inspecting Figure 3, we note a deviation by 25–30 degrees. Explanations of this phenomenon, may perhaps be associated with one of the two particularities of the New Hebrides subduction zone: (1) varying style of deformation along the trench, (2) rotation of the arc.

[22] The first particularity has been described by *Taylor et al.* [1995]. That geodetic study has revealed important

microstructures in the region. GPS measurements in 1990 and 1992 give convergence rate of Australian plate and New Hebrides. In the southern part they measured about 110 mm/yr whereas in the central part they found anomalously low convergence, about the one third of the southern value, this is reflected in the magnitude of the APM calculated at the “eastern” stations (Table S4). They inferred that in the central part cross-arc strike-slip and back-arc reverse faults (CNHCZ = Central New Hebrides Compressional Zone) seem to accommodate the eastward motion of this segment ( $\sim 36$ – $83$  mm/yr) relative to the rest of the arc. Slight differences of observations at arc stations might be due to the different deformation style in the south (extension) and in the north (compression). This may be in relation with the decrease of seismicity under PVC with respect to other arc-located stations. This fact may indicate a change of geometry with latitude. We have inspected this hypothesis, but have not found along-arc variations that are large enough to explain the angular deviation, and its change with latitude.

[23] SKS splitting observations are affected by anisotropy at different depths. Can contributions from the slab and the wedge produce such deviations? Vertical cross sections of areas around the stations indicate that stations sample primarily the sub-slab region: anisotropy under SAN can come from the sub-slab, a contribution to the anisotropic signal could come from the slab under PVC while TAN samples the sub-slab as well as the slab and mantle wedge. The majority of anisotropic signal probably comes from the sub-slab region, but a contribution from the transition zone cannot be excluded, in fact a situation is seen in the adjacent Tonga subduction by *Foley and Long* [2011]. Additional effects might come from the slab and wedge. SAN and PVC stations do not sample the mantle wedge at all thus they could not be affected by processes in the mantle wedge such as the aforementioned variation of deformation style along the trench. In any case, the anisotropy that we might expect in the wedge, the slab, and the sub-slab region does not lend itself easily to explain an oblique alignment of fast directions. Thus one should look for the cause of anisotropy under the slab, for stations PVC, TAN and also LIF.

[24] We are left with asymmetric rotation of the arc as a potential to fully understand the seismic anisotropy this area. As *Schellart et al.* [2006] described, the New Hebrides retreat extremely quickly: the original north-dipping subduction was initiated 10 Ma ago and it rotated to its present location during this time. Asymmetric rollback might produce an internal deformation due to the different degree of shearing along the trench. The shearing might rotate olivine lattice to trench-oblique orientation. Flow induced by rotation might explain why the angular deviation is largest where absolute plate motion is largest. Theoretical investigations have shown that in a rapidly rotating flow, fast directions may attain orientations that have no simple relation with the geometry of flow [e.g., *Kaminski and Ribe*, 2002; *Conrad et al.*, 2007]. If we have captured that phenomenon here, this may give new possibilities of constraining the nature of the flow in the area.

[25] The direction of anisotropy found at station MSVF follows the results given by *Fischer and Wiens* [1996], where a study on the stations belonging to the Tonga subduction zone has been performed. MSVF and the nearby stations present NW orientation of the anisotropic axis, which is almost parallel to the absolute motion of the Pacific

plate; this pattern reflects a subduction-induced back-arc mantle flow field.

#### 4. Conclusions

[26] This study has presented an overview of the results of the first comprehensive SKS shear-wave splitting investigation in the New Hebrides subduction zone. We have attempted to distinguish two types of processes; absolute plate motion and “toroidal” mantle flow for the subducting plate. *Barruol and Hoffmann* [1999] have indicated that this is difficult to do from fast directions alone. However, inspecting splitting delay times one can find that they are close to the average delay time value of splitting measurements from all stations on oceanic islands. This suggests that these anisotropic parameters can be explained without the presence of the subduction zone. Thus, APM appears to explain better the anisotropy observed at the “western” stations. The delay times of “eastern” stations are higher than that of “western” stations. “Eastern” stations are located close to the subduction zone, which suggests that the additional  $\delta t$  may be due to the presence of the subduction zone. Superposition of the effect of APM of Australian plate and of the subduction zone create stronger anisotropy since the strike of the subduction and APM direction are geometrically similar. Therefore, we infer that anisotropy under the “eastern” stations might be due to a combination of APM of the Australian plate and “toroidal” mantle flow behind the slab. Slight deviation from the trench-parallel orientation and differences of anisotropic parameters of “eastern” stations may be caused by one of two particularities of this subduction zone, a) the varying style of deformation along the trench, or b) the fast and asymmetric rotation of the arc.

[27] **Acknowledgments.** We acknowledge M. Pierre Lebellegard from the Laboratoire de Sismologie - Centre IRD de Nouméa who provided us with the Cavascope data very quickly and efficiently, Julien Collot and Bernard Pelletier for providing helpful information on the geology and geodynamics of the area. We also thank Maria Theresia Apoloner for her contribution to Figure 3 and we are also thankful to György Hetényi for his suggestions that improved the manuscript. We thank the anonymous reviewer and Martha Savage for the useful comments to our paper, and are thankful to Nicolas Chamot-Rooke for helpful discussion on the geodynamics of the area.

[28] The Editor thanks the anonymous reviewer and Martha Savage for their assistance in evaluating this paper.

#### References

- Babuska, V., and M. Cara (1991), *Seismic Anisotropy in the Earth*, 217 pp., Kluwer Acad., Norwell, Mass.
- Barruol, G., and R. Hoffmann (1999), Upper mantle anisotropy beneath the Geoscope stations, *J. Geophys. Res.*, *104*(B5), 10,757–10,773, doi:10.1029/1999JB900033.
- Conrad, C. P., M. D. Mark, and P. G. Silver (2007), Global mantle flow and the development of seismic anisotropy: Differences between the oceanic and continental upper mantle, *J. Geophys. Res.*, *112*, B07317, doi:10.1029/2006JB004608.
- Fischer, K. M., and D. A. Wiens (1996), The depth distribution of mantle anisotropy beneath the Tonga subduction zone, *Earth Planet. Sci. Lett.*, *142*, 253–260, doi:10.1016/0012-821X(96)00084-2.
- Foley, B. J., and M. D. Long (2011), Upper and mid-mantle anisotropy beneath the Tonga slab, *Geophys. Res. Lett.*, *38*, L02303, doi:10.1029/2010GL046021.
- Fontaine, F. R., G. Barruol, A. Tommasi, and G. H. R. Bokelmann (2007), Upper-mantle flow beneath French Polynesia from shear wave splitting, *Geophys. J. Int.*, *170*, 1262–1288, doi:10.1111/j.1365-246X.2007.03475.x.
- Fouch, M. J., and K. M. Fischer (1998), Shear wave anisotropy in the Mariana subduction zone, *Geophys. Res. Lett.*, *25*(8), 1221–1224, doi:10.1029/98GL00650.
- Gripp, A. E., and R. G. Gordon (2002), Young tracks of hot-spots and current plate velocities, *Geophys. J. Int.*, *150*, 321–361, doi:10.1046/j.1365-246X.2002.01627.x.
- Heyworth, Z., K. M. Knesel, S. P. Turner, and R. J. Arculus (2011), Pb-isotopic evidence for rapid trench-parallel mantle flow beneath Vanuatu, *J. Geol. Soc.*, *168*, 265–271, doi:10.1144/0016-76492010-054.
- Jung, H., and S. Karato (2001), Water-induced fabric transitions in olivine, *Science*, *293*, 1460–1463, doi:10.1126/science.1062235.
- Kaminski, E., and N. M. Ribe (2002), Timescales for the evolution of seismic anisotropy in mantle flow, *Geochem. Geophys. Geosyst.*, *3*(8), 1051, doi:10.1029/2001GC000222.
- Kennett, B. L. N., and E. R. Engdahl (1991), Traveltimes for global earthquake location and phase identification, *Geophys. J. Int.*, *105*, 429–465, doi:10.1111/j.1365-246X.1991.tb06724.x.
- Long, M. D., and P. G. Silver (2008), The subduction zone flow field from seismic anisotropy: A global view, *Science*, *319*, 315–318, doi:10.1126/science.1150809.
- Long, M. D., and R. D. van der Hilst (2005), Upper mantle anisotropy beneath Japan from shear wave splitting, *Phys. Earth Planet. Inter.*, *151*, 206–222, doi:10.1016/j.pepi.2005.03.003.
- Montagner, J.-P., D.-A. Griot-Pommeroy, and J. Lavé (2000), How to relate body wave and surface wave anisotropy?, *J. Geophys. Res.*, *105*(B8), 19,015–19,027, doi:10.1029/2000JB900015.
- Nakajima, J., and A. Hasegawa (2004), Shear-wave polarization anisotropy and subduction-induced flow in the mantle wedge of northeastern Japan, *Earth Planet. Sci. Lett.*, *225*, 365–377, doi:10.1016/j.epsl.2004.06.011.
- Pillet, R., D. Rouland, G. Roullet, and D. A. Wiens (1999), Crust and upper mantle heterogeneities in the southwest Pacific from surface wave phase velocity analysis, *Phys. Earth Planet. Inter.*, *110*, 211–234, doi:10.1016/S0031-9201(98)00137-X.
- Pillet, R., P. Lebellegard, E. Garaebiti, and D. Rouland (2008), Cavascope: The broadband seismological network of the new Hebrides subduction Zone and its associated data base, *Seismol. Res. Lett.*, *79*(4), 498–503, doi:10.1785/gssrl.79.4.498.
- Savage, M. K. (1999), Seismic anisotropy and mantle deformation: What have we learned from shear wave splitting?, *Rev. Geophys.*, *37*(1), 65–106, doi:10.1029/98RG02075.
- Schellart, W. P., G. S. Lister, and V. G. Toy (2006), A late Cretaceous and Cenozoic reconstruction of the southwest Pacific region: Tectonics controlled by subduction and slab rollback processes, *Earth Sci. Rev.*, *76*, 191–233, doi:10.1016/j.earscirev.2006.01.002.
- Silver, P. G., and W. W. Chan (1988), Implications for continental structure and evolution from seismic anisotropy, *Nature*, *335*, 34–39, doi:10.1038/335034a0.
- Smith, G. P., D. A. Wiens, K. M. Fischer, L. M. Dorman, S. C. Webb, and J. A. Hildebrand (2001), A complex pattern of mantle flow in the Lau Backarc, *Science*, *292*, 713–716, doi:10.1126/science.1058763.
- Taylor, F. W., et al. (1995), Geodetic measurements of convergence at the New Hebrides island arc indicate arc fragmentation caused by an impinging aseismic ridge, *Geology*, *23*, 1011–1014, doi:10.1130/0091-7613(1995)023<1011:GMOCAT>2.3.CO;2.
- Wüstefeld, A., and G. Bokelmann (2007), Null detection in shear-wave splitting measurements, *Bull. Seismol. Soc. Am.*, *97*(4), 1204–1211, doi:10.1785/0120060190.
- Wüstefeld, A., G. Bokelmann, C. Zaroli, and G. Barruol (2008), SplitLab: A shear-wave splitting environment in Matlab, *Comput. Geosci.*, *34*, 515–528, doi:10.1016/j.cageo.2007.08.002.
- Yan, G. Y., and L. W. Kroenke (1993), A plate tectonic reconstruction of the Southwest Pacific, 0–100 My, *Proc. Ocean Drill. Program Sci. Results*, *130*, 697–709.

I. Bianchi, G. Bokelmann, and E. Király, Institute of Meteorology and Geophysics, Universität Wien, Althanstraße 14, UZA II, A-1090 Vienna, Austria. (irene.bianchi@univie.ac.at)